Pergamon

Tetrahedron 55 (1999) 8313–8322

TETRAHEDRON

Experimental and Theoretical Investigations into the Stereoselectivities of Peracid Promoted Epoxidations of Substituted Norbornenes and Norbornadienes

Alan P. Marchand,* Bishwajit Ganguly, Rajesh Shukla, Kasireddy Krishnudu, and V. Satish Kumar

Department of Chemistry, University of North Texas, Denton, Texas 76203-5070

William H. Watson* and Satish G. Bodige

Department of Chemistry, Texas Christan University, Fort Worth, Texas 76129-8860

Received 13 April 1999; revised 27 April 1999; accepted 21 May 1999

Abstract: MCPBA promoted diastereoselective epoxidations of functionalized norbornenes and norbornadienes have been performed. The experimental results thereby obtained have been evaluated by using semiempirical (AM1) quantum chemical modeling. The AM1 computational results are consistent with experiment and correctly predict the major product of all MCPBA promoted epoxidations studied herein. Product characterization was assisted via the results of X-ray crystallographic structural analysis in the case of **10a** and by comparison of calculated *vs.* experimental ^{13}C NMR chemical shifts of the cyclopropyl carbon atoms in **12a** and **12b**.

Keywords: *Oxiranes, Stereoselection, Theoretical studies,*

INTRODUCTION

Peracid promoted epoxidations of alkenes is a familiar and synthetically useful reaction.[1] Bartlett[2] has suggested a "butterfly mechanism" to account mechanistically for the course of reactions of this type. Such epoxidations are generally believed to proceed via a concerted reaction pathway; nevertheless, the timing of formation of the two oxirane C-O bonds and the sequence of events that is involved in C-O bond formation and in hydrogen-transfer remains controversial.[3-7] Recently, Singleton *et al.*[8] have employed high-precision experimental kinetic isotope effect (KIE) data along with the results of high-level theoretical transition structure calculations to define the geometry of the epoxidation transition state. The results thereby obtained suggest that the new oxirane C-O bonds are formed in nearly synchronous fashion.[8]

As part of a continuing study that involves the synthesis and crystal density modeling of polycarbocyclic oxiranes,[9] we have undertaken an experimental and theoretical study of π-facial selectivities that accompany peracid promoted epoxidations of 5,6-disubstituted, 7,7-disubstituted, and 5,6,7,7-tetrasubstituted norbornenes and

*E-mail: marchand@unt.edu; FAX: (940)369-7374.

0040-4020/99/$ - see front matter
PII: S0040-4020(99)00464-0

norbornadienes (Scheme 1). As part of this study, we have employed semiempirical calculations (AM1 Hamiltonian)[11] to predict the preferred reaction pathway by which peracid approaches the norbornene C=C double bonds in each of these substrates during the epoxidation reactions under consideration.

Scheme 1

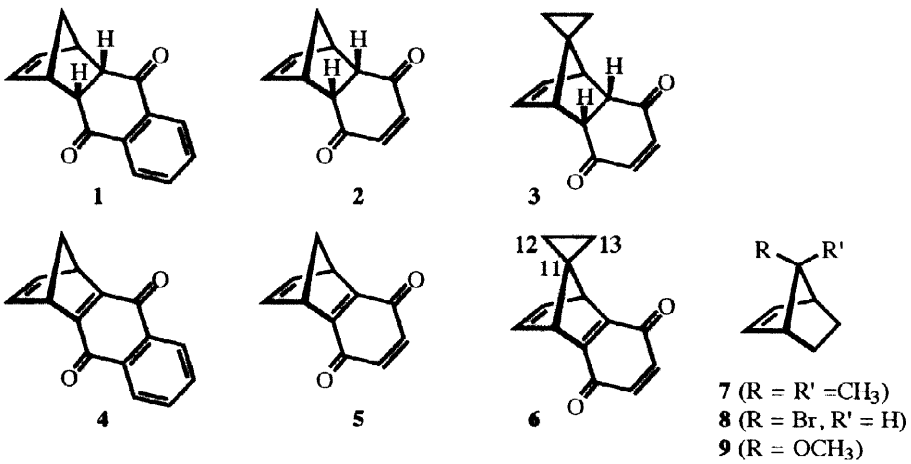

RESULTS AND DISCUSSION

A. Experimental Results. Reaction of a solution of **4**[9c] in CH_2Cl_2 with *m*-chloroperbenzoic acid (MCPBA) at 25 °C resulted in the formation of a mixture of the corresponding epoxides, i.e., **10a** and **10b** (Scheme 2; product ratio **10a** : **10b** = 8: 1). The resulting mixture of isomeric epoxides was separated via column chromatography, and the individual isomers were characterized. The major product of epoxidation of **4** was demonstrated unequivocally to possess structure **10a** via application of X-ray crystallographic methods (see the Experimental Section).

Scheme 2

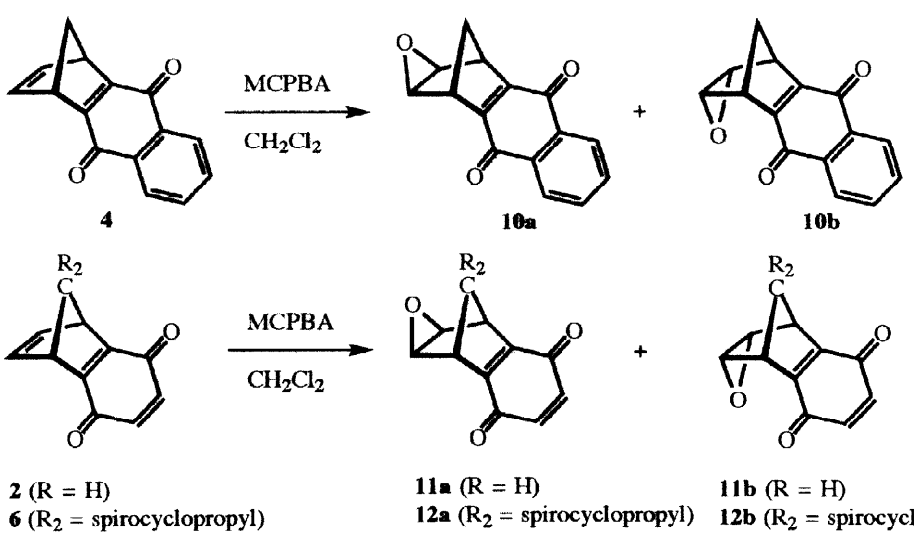

Similarly, MCPBA promoted epoxidation of **5**[10] produced a mixture of epoxides **11a** and **11b** (Scheme 2; product ratio **11a** : **11b** = 3.6 : 1). Once again, the product mixture was separated via column chromatography, and the individual isomers were characterized. Despite considerable effort, we were not able to obtain a good quality single crystal of either isomer; hence, X-ray crystallography could not be employed to determine the structure of either isomer (**11a** or **11b**). Instead, we turned to computational methods in an effort to predict the distribution of products that result via MCPBA promoted epoxidation of **5** (*vide infra*).

MCPBA promoted epoxidation of a solution of **6**[10] in CH_2Cl_2 at 25 °C afforded a mixture of the corresponding epoxides (i.e., **12a** and **12b**, Scheme 2; product ratio **12a** : **12b** = 3 : 2). Our attempts to separate the mixture of products via column chromatography resulted only in the isolation of a minute quantity (*ca.* 10 mg) of the minor epoxidation product, **12b**. Subsequent efforts to obtain a good quality single crystal of **12b** were not successful. In this case, a combination of NMR spectral analysis and computational methods were employed in an effort to account for the observed product distribution (*vide infra*).

B. Computational Results. The relatively large size of the systems of interest effectively precluded the use of high-level ab initio theoretical methods. Accordingly, semempirical molecular orbital computational methods were used to model the transition states for the various epoxidation reactions studied herein. The results thereby obtained could be compared with the corresponding results of previously published B3LYP studies which demonstrated that peracid epoxidations of alkenes proceed via spirocyclic transition states.[8]

The transition state structure was calculated at the AM1 level of theory[11] for performic acid promoted epoxidation of ethylene. The computed transition state structure, i.e., **13a** (Figure 1), indicates that a spirocyclic geometry is adopted in which C-O bonds are formed in synchronous fashion. The approximate plane in the spirocyclic transition state that contains the performic acid moiety is skewed relative to the plane defined by the developing oxirane moiety. The AM1 calculated angle between the two spiro rings was determined to be 88.6°. The geometry of the transition state that was arrived at via semiempirical AM1 calculations is in substantive agreement with the corresponding results calculated at the B3LYP/6-31G* level of theory that were reported previously by Singleton and co-workers.[8]

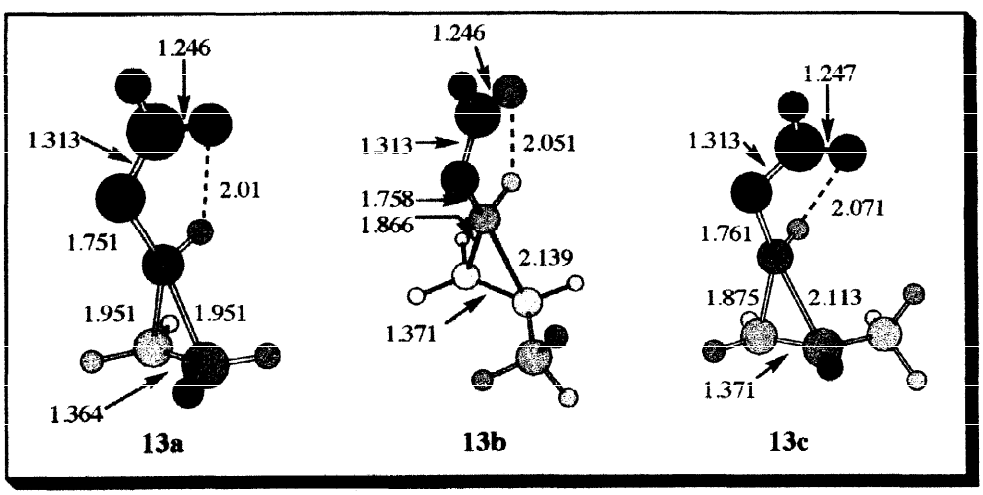

Figure 1. Transition state geometries for performic acid promoted epoxidation of ethylene (**13a**) and propene (**13b** and **13c**). Calculated bond distances are in Å.

The results of the B3LYP/6-31G* computed transition structures for performic acid promoted epoxidation of propene suggest that new C-O bond formation proceeds in slightly *asynchronous* fashion.[8] Interestingly, four transition geometries are predicted by the results of calculations performed at the MP2/6-31G* level of theory for performic acid promoted epoxidation of propene, whereas only two transition states were observed at B3LYP/6-31G* level.[8] The corresponding AM1 results also show asynchronocity for the propene-performic acid transition states. Furthermore, the results of AM1 calculations also lead to only two transition structures for performic acid promoted epoxidation of propene (i.e., **13b** and **13c**, Figure 1).

The observed similarity between B3LYP/6-31G* and AM1 calculated transition state geometries for the foregoing epoxidation reactions encouraged us to continue to utilize the much less time-intensive AM1 calculations as a means to predict stereoselectivities in performic acid promoted epoxidations of more complex, π-facially differentiated alkenes. To this end, we next examined a series of substituted norbornenes and norbornadienes as epoxidation substrates.

The fact that a spirocyclic transition state is predicted for peracid promoted oxidation of alkenes suggests that there will be two possible transition states that correspond to each mode of approach by peracid toward the *exo*- and *endo*-π-face of a C=C double bond in norbornenes and norbornadienes. The lower energy of the two transition states obtained for each mode of π-facial attack by peracid will be compared.

The AM1 calculated transition states for performic acid promoted epoxidations of norbornene and norbornadiene are shown in Figure 2. Here, it can be seen that the calculated transition state geometries for all four possible transition states are slightly asynchronous. The extent of asynchronicity of C-O bond formation therein is seen to be somewhat more pronounced for *exo* than for *endo* approach by the oxidant in both cases studied.

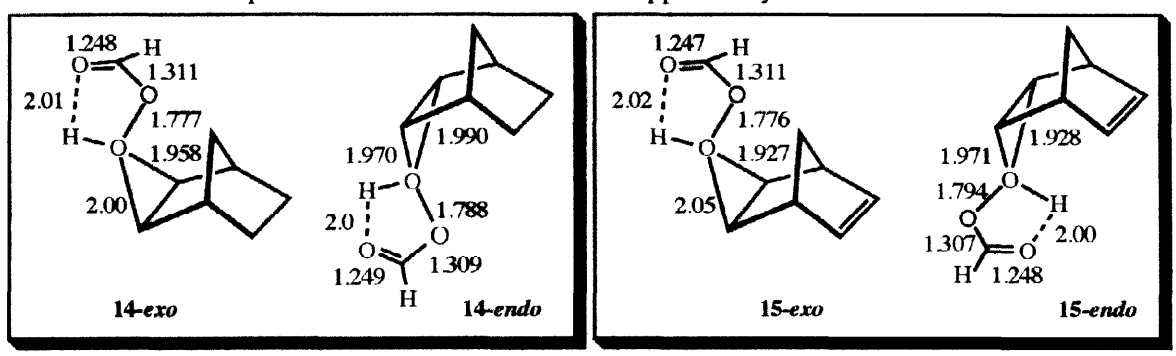

Figure 2: AM1 calculated transition states for performic acid peroxidation of norbornene (**14-*exo*** and **14-*endo***) and norbornadiene (**15-*exo*** and **15-*endo***).

Peracid promoted epoxidations of norbornene and norbornadiene, like most electrophilic additions to the C=C double bonds in these systems, usually proceed via predominant (or even exclusive) approach of the oxidant toward the *exo* face of the substrate.[12] In agreement with this experimental observation,[13] we find that the calculated (AM1) $\Delta E = E_{exo} - E_{endo}$ value for diastereoisomeric transition states **14-*exo*** and **14-*endo*** is -1.6 kcal-mol^{-1}, while the corresponding calculated ΔE value for diastereoisomeric transition states **15-*exo*** and **15-*endo*** is -1.9 kcal-mol^{-1}.

However, in contrast to the behavior of norbornene and norbornadiene, MCPBA promoted oxidation of 7,7-dimethylnorborn-2-ene (**7**) and of *syn*-7-bromonorbornene (**8**) both proceed with predominant approach of the electrophilic epoxidizing agent upon the *endo* π-face of the C=C double bond in the substrate.[14] Once again,

this experimental observation is borne out by the results of AM1 calculations; here, we find that the calculated (AM1) $\Delta E = E_{exo} - E_{endo}$ values for these diastereoisomeric transition states are +2.5 and +4.6 kcal-mol^{-1}, respectively.

This same computational approach then was applied to performic acid promoted epoxidations of substrates **1-6** and **9** (Scheme 1). In this connection, it should be noted that MCPBA promoted epoxidations of **1**,[9c] **2**,[15] and **3** [9b] and **9**[16] have been reported to proceed with exclusive formation of the corresponding *exo*-epoxide, in each case. In the present study, we find that the corresponding MCPBA promoted epoxidations of **4**, **5**, and **6** all afford a mixture of *exo* and *endo* epoxides in which the *exo* product predominates (*vide supra*).

Transition state calculations have been performed at the AM1 level of theory by using performic acid as a model for MCPBA. The results of these calculations are summarized in Table 1. The results thereby obtained for **1-6** indicate that epoxidation should occur preferentially upon the *exo* face of each substrate. Thus, the transition state for *exo* epoxidation is predicted on the basis of AM1 computational results to be preferred energetically *vis-à-vis* that for the corresponding *endo* epoxidation in **1-3** by -9.6, -8.0, and -4.4 kcal-mol^{-1}, respectively. In comparison, the corresponding preference for *exo* epoxidation in **4-6** is somewhat lower (i.e., -3.9, -3.3, and -1.2 kcal-mol^{-1}, respectively), in agreement with experimental observations.

Table 1. Calculated (AM1) transition state energy differences, $\Delta E = E_{exo} - E_{endo}$, in kcal-mol^{-1}, for performic acid promoted epoxidations of substituted norbornenes and norbornadienes.

Substrate	$\Delta E = E_{exo} - E_{endo}$ (kcal-mol^{-1})
norbornene	-1.7
norbornadiene	-1.9
1	-9.6
2	-8.0
3	-4.4
4	-3.9
5	-3.3
6	-1.2
7	+2.5
8	+4.6
9	-1.7

Interestingly, the cyclopropyl spiroannulation (as in **3** and **6**) reduces the *exo*/*endo* epoxidation ratio. However, this effect is not nearly as pronounced as the corresponding effect of methylation or bromination (as in **7** and **8**), which is sufficient to reverse the *exo*/*endo* epoxidation selectivity.[14] Once again, the calculated AM1 results (Table 1) qualitatively support experimental observations.

Finally, the results of transition state calculations for performic acid promoted epoxidation of 7,7-dimethoxynorbornene (**9**, Table 1) indicate that approach by the oxidizing agent toward the *exo* face of **9** is preferred energetically over the corresponding *endo* face approach, a prediction that is borne out by experiment.[16] In contrast to this result, it was noted above that the corresponding reaction of 7,7-dimethylnorbornene (**7**) proceeds via pre-

dominant attack of the oxidizing agent upon the *endo* face of the substrate (*vide supra*). It is tempting to ascribe the observed differences in behavior of these two substrates toward epoxidizing agents to the operation of hydrogen bonding by the *syn*-OCH_3 substituent in **9**, which helps to direct the incoming electrophilic oxidizing agent toward the *exo* face of the substrate.[16] The AM1 calculated *exo* transition state geometry indicates that the peracid -OOH hydrogen atom forms a hydrogen bond with the *syn*-OMe oxygen atom in **9** (Figure 3). Similar substrate-directed effects in the epoxidation of allyl alcohol with performic acid have been reported.[17]

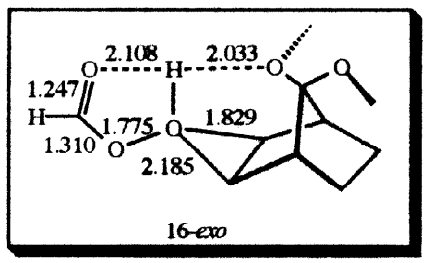

Figure 3: AM1 calculated *exo* transition state for performic acid epoxidation of 7,7-dimethoxynorbornane.

^{13}C Spectral assignments for compound 12a and 12b: As noted above, MCPBA promoted epoxidation of **6** afforded a mixture of the corresponding epoxides (i.e., **12a** and **12b**, Scheme 2; product ratio **12a** : **12b** = 3 : 2). Structural assignment of each of these epoxidation products was achieved via analysis of their respective ^{13}C NMR spectra.

It was noted that the ^{13}C NMR chemical shifts of the cyclopropyl carbon atoms differ significantly in **12a** and **12b**. *Gaussian 94*[18a] has been employed to calculate the ^{13}C NMR chemical shifts of the cyclopropyl carbon atoms in these systems by using gauge-independent atomic-orbital (GIAO) computational methodology.[18b] The ^{13}C NMR chemical shifts for **12a** and **12b** have been calculated at the hybrid *ab initio* HF-DFT B3LYP/6-311+G** level of theory.[19] The calculated chemical shifts thereby obtained appear in Table 2, where they are expressed in parts per million (δ) downfield from the corresponding isotropic ^{13}C NMR chemical shift calculated for tetramethylsilane (TMS) at the same level of theory. The cyclopropyl carbon atom numberings are shown in Scheme 1.

Table 2. B3LYP/6-311+G** calculated and experimentally observed ^{13}C NMR chemical shifts for the products formed via MCPBA promoted epoxidation of **6**

Cyclopropyl carbon atom number	**δ(12a) / δ(12b) (PPM, calculated)**	**δ(major product) / δ(minor product) (PPM, observed)**
C(11)	47.1 / 65.0	39.8 / 58.2
C(12)	2.7 / 9.1	0.4 / 6.90
C(13)	14.8 / 6.6	11.9 / 5.2

As can be seen by inspection of the data in Table 2, the trend shown by the calculated ^{13}C NMR chemical shifts for the cyclopropyl carbon atoms in **12a** and **12b** are in good agreement with experiment. Based upon these ^{13}C chemical shifts assignments, we feel confident in assigning structure **12a** (rather than **12b**) to the major

product of MCPBA promoted epoxidation of **6**.[20] Furthermore, the results of our AM1-level transition state calculations support this conclusion.

SUMMARY AND CONCLUSIONS

The AM1 calculated transition states geometries for performic acid promoted epoxidation of ethylene and propene are consistent with those derived from the corresponding results of previously published[8] B3LYP/6-31G* calculations. In the present study, a simple AM1-derived computational model was used to predict the course of MCPBA promoted epoxidations of several π-facially differentiated alkenes. The predictions based upon the AM1 model have been found to be qualitatively in good agreement with previously published experimental results and also with those obtained in the present study for MCPBA promoted epoxidations of compounds **4-6**. Cyclopropyl spiroannulation was found to reduce the *exo* stereoselectivity of MCPBA promoted epoxidation of **3** and **6** *vis-à-vis* that of **2** and **5**, respectively. However, this effect is not as pronounced as the corresponding effect produced by *syn*-CH_3 and *syn*-Br, as in systems **7** and **8**, both of which are predicted (AM1) to undergo stereoselective epoxidation that results via approach of the peracid upon the *endo* π-face of the norbornene C=C double bond, in agreement with experiment.[14] Finally the results of AM1 calculations permit us to rationalize the observed preference of 7,7-dimethoxynorbornane to undergo stereoselective MCPBA promoted *exo* epoxidation in terms of selective stabilization of the *exo* transition state via intramolecular hydrogen bonding.

EXPERIMENTAL SECTION

Melting points are uncorrected. ^1H and ^{13}C NMR spectra were obtained at 200 MHz and 50 MHz, respectively, by using a Varian Gemini 200 nuclear magnetic resonance spectrometer. Infrared spectra were obtained on a Midac Model 100 FTIR spectrophotometer. High-resolution mass spectral data reported herein for **12b** were obtained by Professor Jennifer S. Brodbelt at the Mass Spectrometry Facility at the Department of Chemistry and Biochemistry, University of Texas at Austin by using a ZAB-E double sector high-resolution mass spectrometer (Micromass, Manchester, England) that was operated in the chemical ionization mode. Elemental microanalytical data were obtained by personnel at M-H-W Laboratories, Phoenix, AZ.

Epoxidation of 4. A solution of **4**[9c] (250 mg, 1.12 mmol) in CH_2Cl_2 (25 mL) was pre-cooled to 0-5 °C via application of an external ice-water bath. To this cooled solution was added dropwise with stirring MCPBA (251 mg, 1.45 mmol) in CH_2Cl_2 (5 mL), and the resulting mixture was stirred at 0-5 °C for 0.5 h. The external cold bath was removed, and the reaction mixture was allowed to warm gradually to ambient temperature with stirring during 24 h. The reaction mixture was washed sequentially with saturated aqueous $NaHCO_3$ (5 × 10 mL) and water (2 × 25 mL), dried ($MgSO_4$) and filtered, and the filtrate was concentrated *in vacuo*. The residue (181 mg, 67%) was purified via column chromatography on silica gel by eluting with 20% EtOAc-hexane. Workup of the first chromatography fraction afforded pure **10a** (160 mg, 60%) as a colorless microcrystalline solid: mp 148-149 °C; IR (KBr) 3005 (w), 2976 (w), 1665 (s), 1591 (s), 1298 (s), 850 (s) cm^{-1}; ^1H NMR ($CDCl_3$) δ 1.59 (broadened *AB*, J_{AB} = 9.0 Hz, 1 H), 1.96 [t(A*B*), J_{AB} = 9.0 Hz, *J*=2.1 Hz, 1 H], 3.58 (s, 2 H), 3.69 (m, 2 H), 7.64-7.73 (m, 2 H), 8.00-8.11 (m, 2 H); ^{13}C NMR ($CDCl_3$) δ 39.5 (t), 42.8 (d), 57.6 (d), 126.3 (d), 132.6 (s), 133.6 (d), 159.7 (s), 181.7 (s). Anal. Calcd for $C_{15}H_{10}O_3$: C, 75.62; H, 4.23. Found: C, 75.30; H, 4.09.

Continued elution of the chromatography column afforded a second fraction. Workup of the second chromatography fraction afforded the minor reaction product, i.e., **10b** (21 mg, 8%) as a colorless microcrystalline solid: mp 152-153 °C; IR (KBr) 3004 (w), 2973 (w), 1665 (s), 1590 (s), 1296 (s), 851 (s) cm^{-1}; ^1H NMR ($CDCl_3$) δ 2.23 (broadened *AB*, J_{AB} = 9.0 Hz, 1 H), 2.34 [t(A*B*), J_{AB} = 9.0 Hz, *J*=1.7 Hz, 1 H], 3.55 (broadened

quintet, J=1.5 Hz, 2 H), 3.93 (d, J=1.2 Hz, 2 H), 7.62-7.71 (m, 2 H), 8.04-8.10 (m, 2 H); ^{13}C NMR ($CDCl_3$) δ 42.6 (t), 53.5 (d), 60.9 (t), 126.8 (d), 133.4 (s), 133.9 (d), 149.5 (s), 182.5 (s). Anal. Calcd for $C_{15}H_{10}O_3$: C, 75.62; H, 4.23. Found: C, 75.37; H, 4.26.

Epoxidation of 5. A solution of **5**[10] (300 mg, 1.59 mmol) in CH_2Cl_2 (20 mL) was pre-cooled to 0-5 °C via application of an external ice-water bath. To this cooled solution was added dropwise with stirring MCPBA (411 mg, 2.30 mmol) in CH_2Cl_2 (5 mL), and the resulting mixture was stirred at 0-5 °C for 0.5 h. The cold bath was removed, and the reaction mixture was allowed to warm gradually to ambient temperature with stirring during 24 h. During this time, the progress of the reaction was monitored via thin layer chroma-tographic (tlc) analysis. The reaction was quenched via addition of 10% aqueous $NaHCO_3$ (60 mL), and the resulting aqueous suspension was extracted with CH_2Cl_2 (3 × 20 mL). The combined organic extracts were washed sequentially with water (3 × 10 mL) and brine (20 mL), dried ($MgSO_4$) and filtered, and the filtrate was concentrated *in vacuo*. The residue (179 mg, 55%) was purified via column chromatography on silica gel by eluting with 20% EtOAc-hexane. Workup of the first chromatography fraction afforded pure **11a** (140 mg, 42.6%) as a colorless microcrystalline solid: mp 118-119 °C; IR (KBr) 2963 (w), 1685 (s), 1671 (s), 1567 (w), 1388 (w), 1284 (w), 849 (m) cm^{-1}; ^{1}H NMR (benzene-d_6) δ 0.84 [t(*AB*), J_{AB} = 6.0 Hz, J=1.0 Hz, 1 H], 1.61 [t(A*B*), J_{AB} = 6.0 Hz, J=1.0 Hz, 1 H], 2.86 (s, 2 H), 3.10 (m, 2 H), 5.94 (s, 2 H); ^{13}C NMR (benzene-d_6) δ 40.4 (t), 43.06 (d), 58.1 (d), 136.4 (d), 157.9 (s), 184.3 (s); Anal. Calcd for $C_{11}H_8O_3$: C, 70.21; H, 4.28. Found: C, 70.33; H, 4.27.

Continued elution of the chromatography column afforded a second fraction. Workup of the second chromatography fraction afforded the minor reaction product, i.e., **11b** (39 mg, 12%) as a colorless microcrystalline solid: mp 190-191 °C; IR (KBr) 3039 (w), 1664 (s), 1298 (w), 1056 (w), 876 (m) cm^{-1}; ^{1}H NMR (benzene-d_6) δ 2.18 [t(*AB*), J_{AB} = 9.0 Hz, J=1.2 Hz, 1 H], 2.30 [t(A*B*), J_{AB} = 9.0 Hz, J=1.8 Hz, 1 H], 3.43 (broadened quintet, J= 1.0 Hz, 2 H), 3.89 (d, J = 3.0 Hz, 2 H), 6.63 (s, 2 H); ^{13}C NMR (benzene-d_6) δ 42.2 (t), 53.2 (d), 61.0 (d), 136.6 (d), 147.0 (s), 184.8 (s); Anal. Calcd for $C_{11}H_8O_3$: C, 70.21; H, 4.28. Found: C, 69.97; H, 4.27.

Epoxidation of 6. A solution of **6**[10] (200 mg, 1.00 mmol) in CH_2Cl_2 (20 mL) was pre-cooled to 0-5 °C via application of an external ice-water bath. To this cooled solution was added dropwise with stirring MCPBA (241 mg, 1.40 mmol) in CH_2Cl_2 (5 mL), and the resulting mixture was stirred at 0-5 °C for 0.5 h. The external cold bath was removed, and the reaction mixture was allowed to warm gradually to ambient temperature with stirring during 24 h. During this time, the progress of the reaction was monitored via thin layer chroma-tographic (tlc) analysis. The reaction was quenched via addition of 10% aqueous $NaHCO_3$ (30 mL), and the resulting aqueous suspension was extracted with CH_2Cl_2 (3 × 10 mL). The combined organic extracts were washed sequentially with water (3 × 10 mL) and brine (20 mL), dried ($MgSO_4$) and filtered, and the filtrate was concentrated *in vacuo*. The residue (140 mg, 65%) was purified via column chromatography on silica gel by eluting with 20% EtOAc-hexane. Workup of the first chromatography fraction afforded a mixture of **12a** and **12b**. We were unable to isolate isomerically pure **12a** from the crude reaction product mixture via column chromatographic purification; ^{1}H NMR of a mixture of **12a** and **12b** ($CDCl_3$) δ 0.21-0.29 (m, 1.2 H), 0.43-0.51 (m, 0.8 H), 0.69-0.77 (m, 0.8 H), 0.79-0.88 (m, 1.2 H), 2.97 (d, J = 3.2 Hz, 0.4 H), 3.14 (s, 0.6 H), 3.66 (s, 0.6 H), 3.98 (d, J = 3.3Hz, 0.4 H), 6.65 (br s, 2 H); ^{13}C NMR ($CDCl_3$) δ 0.43 (t), 5.2 (t), 6.9 (t), 11.9 (t), 39.8 (s), 48.0 (d), 49.9 (d), 52.4 (d), 58.1 (s), 59.7 (d) 136.3 (d), 136.6 (d), 146.7 (s), 157.6 (s), 184.2 (s), 184.6 (s).

Continued elution of the chromatography column afforded a second fraction. Workup of the second chromatography fraction afforded the minor reaction product, isomerically pure **12b** (10 mg, 5%) as a colorless microcrystalline solid: mp 240-241 °C; IR (KBr) 1647(s), 1322 (s), 1097 (s), 836 (s) cm^{-1}; ^{1}H NMR ($CDCl_3$) δ 0.43-0.51 (m, 2 H), 0.69-0.77 (m, 2 H), 2.97 (t, J = 1.6 Hz, 2 H), 3.98 (d, J = 3.3 Hz, 2 H), 6.65 (br s, 2 H); ^{13}C NMR ($CDCl_3$) δ 5.2 (t), 6.9 (t), 48.0 (d), 52.4 (d), 58.1 (s), 136.6 (d), 146.7 (s), 184.6 (s). Exact mass (CI HRMS) Calcd for $C_{13}H_{10}O_3$: $[M_r + H]^+$ 215.07082. Found: $[M_r + H]^+$ 215.07127.

X-ray Structure Determination of 10a. All data were collected at 23 ± 1 °C on a Rigaku AFC6S diffractometer with graphite monochromated Cu Kα radiation (λ = 1.54178 Å) by using the ω–2θ scan technique with multiple scans for weak reflections. Pertinent X-ray data are given in Table 3. An empirical absorption

correction based on azimuthal scans of several reflections was applied, which resulted in transmission factors ranging from 0.92 to 1.00. Data were corrected for Lorentz and polarization effects. The structure was solved by direct methods (SHELXS86)[21] and was refined and was expanded by using Fourier techniques (DIRDIF94).[22] The non-hydrogen atoms were refined anisotropically. Hydrogen atoms were included but not refined. Neutral atom scattering factors were taken from Cromer and Waber.[23] All calculations were performed by using *teXsan*.[24]

Table 3. X-ray data collection and processing parameters for **10a**

Formula	$C_{15}H_{10}O_3$	γ (°)	90	Unique reflections	2412
Size (mm)	0.20 x 0.30 x 0.40	V (Å^3)	1101.9 (4)	R_{int}	0.025
Space Group	$P2_1/c$	Z-value	4	Observed Reflections $I \geq 3\sigma(I)$	1727
a (Å)	11.645 (2)	D_{calc} (g-cm^{-3})	1.436	Parameters	325
b (Å)	8.700 (3)	μ (cm^{-1})	8.25	R, R_w	0.140, 0.101
c (Å)	11.736 (2)	T (K)	296	$(\Delta/\sigma)_{max}$	0.00
α (°)	90	$2\theta_{max}$ (°)	157.0	ρ_{max}; ρ_{min} (eÅ^{-3})	0.25; -0.24
β (°)	112.06 (1)	Total reflections	2526		

Acknowledgment. We thank the Office of Naval Research [Grant N00014-98-1-0478 (A. P. M.) and The Robert A. Welch Foundation [Grants B-0963 (A. P. M.) and P-0074 (W. H. W.)] for financial support.

REFERENCES AND FOOTNOTES

1. For a review of peracid promoted epoxidation of alkene C=C double bonds, see: Jacobsen, E. N. In *Catalytic Asymmetric Synthesis*, Ojima, I., Ed.; VCH: New York, 1993; Chapter 4.2.

2. Bartlett, P. D. *Rec. Chem. Progr.* **1950**, *11*, 47

3. Hanzlik, R. P.; Shearer, G. O. *J. Am. Chem. Soc.* **1975**, *97*, 5231.

4. Plesnicar, B.; Tasevski, M.; Azman, A. *J. Am. Chem. Soc.* **1978**, *100*, 743.

5. Bach, R. D.; Winter, J. D.; McDougall, J. J. W. *J. Am. Chem. Soc.* **1995**, *117*, 8586.

6. Yamabe, S.; Kondou, C.; Minato, T. *J. Org. Chem.* **1996**, *61*, 616.

7. Lynch, B. M.; Pausacker, K. H. *J. Chem. Soc.* **1955**, 1525.

8. Singleton, D. A.; Merrigan, S. R.; Liu, J.; Houk, K. N. *J. Am. Chem. Soc.* **1997**, *119*, 3385.

9. (a) Marchand, A. P.; Vidyanand, D.; Liu, Z.; Kumar, K. A.; Watson, W. H.; Kashyap, R. P.; Ammon, H. L.; Du, Z. *Tetrahedron* **1996**, *52*, 9703. (b) Marchand, A. P.; Shukla, R.; Davey, P. R. J.; Ammon, H. L.; Du, Z.; Bott, S. G. *Tetrahedron* **1998**, *54*, 4485. (c) Marchand, A. P.; Dong, E. Z.; Bott, S. G. *Tetrahedron* **1998**, *54*, 4459.

10. Marchand, A. P.; Alihodzic, S.; Shukla, R. *Synth. Commun.* **1998**, *28*, 541.

11. (a) Dewar, M. J. S.; Zoebisch, E. G. Zoebisch; Healy, E. F.; Stewart, J. J. P. *J. Am. Chem. Soc.*, **1985**, *107*, 3902. (b) *SPARTAN* version 4.0, 1995; Wavefunction, Inc., 18401 Von Karman Ave., #370, CA 92715. Complete vibrational analysis was performed to characterize each of the transition states.

12. (a) Christol, H.; Coste, J.; Plenat, F. *Tetrahedron Lett.* **1972**, 1143. (b) Christol, H.; Coste, J.; Plenat, F. *Bull. Soc. Chim. France* **1973**, 1064. (c) Davis, D. D.; Surmitis, A. J.; Robertson, G. L.; *J. Organometal. Chem.* **1972**, C(9), 46. (d) Zimmermann, D.; Reisse, J.; Coste, J.; Plenat, F.; Christol, H. *Org. Magn. Reson.* **1971**, *6*, 492.

13. Meinwald, J.; Labana, S. S.; Labana, L. L.; Wahl, G. H., Jr. *Tetrahedron Lett.* **1965**, 1789.

14. (a) Brown, H. C.; Kawakami, J. H.; Ikegami, S. I. *J. Am. Chem. Soc.*, **1970**, *92*, 6914. (b) Zefirov, N. S.; Kasyan. L. I.; Gnedenkov, L. Yu.; Shashkov, A. S.; Cherepaniva, E. G.; *Tetrahedron Lett.* **1979**, 949.

15. Marchand, A. P.; Reddy, G. M. *Tetrahedron*, **1990**, *46*, 3409.

16. Gassman, P. G.; Marshall, J. L. *J. Am. Chem. Soc.* **1966**, *88*, 2822.

17. Bach, R. D.; Estevez, C. M.; Winter, J. E.; Glukhovtsev, M. N. *J. Am. Chem. Soc.* **1998**, *120*, 680.

18. (a) Frisch, M. J.; Trucks, G. W.; Schlegel, H. B.; Gill, P. M. W.; Johnson, B. G.; Robb, M. A.; Cheeseman, J. R.; Keith, T. A.; Petersson, G. A.; Montgomery, J. A.; Raghavachari, K.; AlLatham, M. A.; Zakrzewski, V. G.; Ortiz, J. V.; Foresman, J. B.; Cioslowski, J.; Stefanov, B. B.; Nanayakara, A.; Challacombe, M.; Reng, C. Y.; Ayala, P. Y.; Chen, W.; Wong, M. W.; Andres, J. L.; Replogle, E. S.; Gomperts, R.; Martin, R. L.; Fox, D. J.; Binlley, J. S.; Defrees, D. J.; Baker, J.; Stewart, J. J. P.; Head-Gordon, M.; Gonzalez, C.; Pople, J. A. *Gaussian 94*; Gaussian Inc.; Pittsburgh, PA. 1995. (b) Wolinski, K.; Hilton, J. F.; Pulay, P. *J. Am. Chem. Soc.* **1990**, *112*, 8251.

19. (a) Becke, A. D.; J. *Chem. Phys.* **1993**, *98*, 5648. (b) Becke, A. D. *J. Chem. Phys.* **1996**, *104*, 1040.

20. It should be noted that substituent effects exerted by the oxirane ring on ^{1}H chemical shifts and also the magnitudes of vicinal and long-range ^{1}H-^{1}H spin-spin couplings have been used to assign *exo/endo* stereochemistry in *exo*- and *endo*-2,3-epoxynorbornanes. See: (a) Tori, K.; Kitahonoki, K.; Takano, Y.; Tanida, H.; Tsuji, T. *Tetrahedron Lett.* **1964**, 449. (b) Tori, K.; Aono, K. Kitahonoki, K. Muneyuki, R.; Takano, Y.; Tanida, H.; Tsuji, T. *Tetrahedron Lett.* **1966**, 2921.

21. *SHELXS86:* Sheldrick, G. M. In: *Crystallographic Computing 3*, Sheldrick, G. M.; Kruger, C.; Goddard, R., Eds.; Oxford University Press: Oxford, 1985, pp. 175-189.

22. *DIRDIF94:* Beurskens, P. T.; Admiraal, G.; Beurskens, G.; Bosman, W. P.; de Gelder, R.; Israel, R.; Smits, J. M. M. *The DIRDIF Program System*, Technical Report of the Crystallography Laboratory, University of Nijmegen, The Netherlands, 1994.

23. Cromer, D. T.; Waber, J. T. *International Tables for X-ray Crystallography*, Vol. IV, 1974, Kynoch Press: Birmingham, Table 2.2 A.

24. *teXsan for Windows: Crystal Structure Analysis Package*, Molecular Structure Corp., 1997.